Complete Mitochondrial Genomes and Phylogenetic Positions of Two Longicorn Beetles, *Anoplophora glabripennis* and *Demonax pseudonotabilis* (Coleoptera: Cerambycidae)

De-Qiang Pu [1],*, Hong-Ling Liu [1], Xing-Long Wu [1] and Zhi-Teng Chen [2]

1 Key Laboratory of Integrated Pest Management of Southwest Crops, Institute of Plant Protection, Sichuan Academy of Agricultural Sciences, Chengdu 610066, China
2 School of Grain Science and Technology, Jiangsu University of Science and Technology, Zhenjiang 212004, China
* Correspondence: 201900000027@just.edu.cn

Abstract: *Anoplophora glabripennis* (Motschulsky, 1854) and *Demonax pseudonotabilis* Gressitt & Rondon, 1970 are two commonly found longicorn beetles from China. However, the lack of sufficient molecular data hinders the understanding of their evolution and phylogenetic relationships with other species of Cerambycidae. This study sequenced and assembled the complete mitochondrial genomes of the two species using the next-generation sequencing method. The mitogenomes of *A. glabripennis* and *D. pseudonotabilis* are 15,622 bp and 15,527 bp in length, respectively. The mitochondrial gene content and gene order of *A. glabripennis* and *D. pseudonotabilis* are highly conserved with other sequenced longicorn beetles. The calculation of nonsynonymous (Ka) and synonymous (Ks) substitution rates in PCGs indicated the existence of purifying selection in the two longicorn beetles. The phylogenetic analysis was conducted using the protein-coding gene sequences from available mitogenomes of Cerambycidae. The two species sequenced in this study are, respectively, grouped with their relatives from the same subfamily. The monophyly of Cerambycinae, Dorcasominae, Lamiinae, and Necydalinae was well-supported, whereas Lepturinae, Prioninae, and Spondylidinae were recovered as paraphyletic.

Keywords: Cerambycidae; mitogenome; longicorn beetle; gene arrangement; phylogeny

1. Introduction

Cerambycidae (longicorn beetle) is one of the most speciose families of Coleoptera, comprising over 4000 genera and 35,000 species worldwide [1–3]. Cerambycidae *sensu stricto* (*s.s.*) usually consists of the eight subfamilies: Cerambycinae, Dorcasominae, Lamiinae, Lepturinae, Necydalinae, Parandrinae, Prioninae, and Spondylidinae [4]. Cerambycidae *sensu lato* (*s.l.*) comprises Cerambycidae *s.s.*, Disteniidae, Oxypeltidae, and Vesperidae [5]. The adults of longicorn beetles are morphologically diverse and phytophagous, usually feeding on living plant tissue, pollen, fruit, or tree sap [6]. Larvae of longicorn beetles usually have reduced or sometimes absent legs and they are mostly internal borers of their host plants [7–10]. In cultivated ecosystems, e.g., forest farms and tea gardens, the longicorn beetles are nonnegligible pests causing significant economic damage to the host plants [11,12].

The phylogeny and early evolution of Cerambycidae have been comprehensively reviewed by Haddad & Mckenna (2016) [13]. The phylogeny of longicorn beetles, especially the monophyly of Cerambycidae *s.s.* and *s.l.*, as well as the subfamily and tribe-level relationship, remains debatable due to the high species richness and highly variable morphological characters [5,14,15]. Haddad et al. (2018) [5] reconstructed the higher-level phylogeny of Cerambycidae with anchored hybrid enrichment of nuclear genes. Their results recovered a monophyletic Cerambycidae *s.s.* in most analyses and a polyphyletic

Cerambycidae *s.l.* as well as the monophyletic subfamilies of Cerambycidae *s.s.* except for the paraphyletic Cerambycinae [5]. Nie et al. (2020) [15] used 151 mitochondrial genomes (mitogenomes) representing all families of Chrysomeloidea and all subfamilies of Cerambycidae *s.s.* to explore the higher-level phylogeny of Chrysomeloidea, especially Cerambycidae and allied families. However, their study could not support the monophyly of Cerambycidae *s.s.* and all its subfamilies. The two subfamilies, Necydalinae and Parandrinae, were considered as tribes Necydalini and Parandrini, respectively [15]. Meanwhile, the mitogenomes of many important cerambycid clades remained poorly represented, which restricted the accuracy of the results.

The mitogenome is an informative molecular marker for taxonomic and evolutionary research and has become one of the most popular molecules used in current insect phylogenetic studies [16]. The development of next-generation sequencing techniques largely reduced the expense and experimental period to efficiently obtain the mitogenomes from all kinds of organisms. Diverse insect orders, such as Coleoptera [17,18], Lepidoptera [19], Hemiptera [20], etc., have combined the mitogenomes with dense taxon sampling to generate large-scale phylogenomic datasets for phylogenetic reconstruction and have revealed the strengths of mitogenomes in resolving the higher-level phylogenetic relationships. However, the available number of mitogenomes of Cerambycidae *s.l.* in the NCBI database is out of proportion to the remarkable species richness of longicorn beetles, which is a major impediment to better understanding the classification and evolution of this ecologically and economically significant group of insects.

To provide more genetic data for the longicorn beetles and investigate their phylogenetic relationships, this study sequenced and analyzed the mitogenomes of two commonly found longicorn beetles from China, *A. glabripennis* and *D. pseudonotabilis* [21,22]. Although the mitogenome of *A. glabripennis* (NC_008221) has been sequenced in a previous study [23], it is still very important to sequence more mitogenomes for the same species already listed in GenBank considering the existence of intraspecific variation of mitogenomes between different geographic populations [24]. Phylogenetic trees of Cerambycidae *s.l.* is constructed based on the newly sequenced as well as the known mitogenomic data to investigate the phylogenetic positions of the two newly sequenced species and provide more information for resolving the relationships within Cerambycidae *s.l.*

2. Materials and Methods

2.1. Sample Collection, DNA Extraction, and Mitogenome Sequencing

Adult specimens of *A. glabripennis* and *D. pseudonotabilis* were collected by Malaise traps set in the tea garden of Hongyan Town (29°59′31.42″ N, 103°10′34.45″ E), Mingshan County, Ya'an City, Sichuan Province of China, in 2016. The specimens were identified based on the morphological characteristics under a light microscope and were deposited in Sichuan Academy of Agricultural Sciences (specimen voucher: SAASCO1 (*A. glabripennis*) and SAASCO2 (*D. pseudonotabilis*)). All experiments and procedures for this study complied with the current animal ethics guidelines and did not involve any protected animals.

The total genomic DNA was extracted by E.Z.N.A. Tissue DNA Kit (Omega, Norcross, GA, USA). At least 1 μg of purified DNA was used to construct the TruSeq DNA library with an insert size of 400 bp according to standard protocols. The library was sequenced using the Illumina HiSeq 4000 platform (Personal Gene Technology Co., Ltd., Nanjing, China) with paired-end reads of 2 × 150 bp. A total of 21,616,708 and 22,096,010 raw reads were obtained for *A. glabripennis* and *D. pseudonotabilis*, respectively. Over 97.8% of bases in the raw reads were regarded as correctly identified with an accuracy rate above 99%. The unpaired, short, and low-quality raw reads were filtered by fastp [25] to obtain clean reads. The above quality-control and data-filtering process generated 21,584,444 and 22,059,322 high-quality reads for *A. glabripennis* and *D. pseudonotabilis*, respectively.

2.2. Mitogenome Assembly, Annotation, and Analyses

Before the assembly, the high-quality reads were trimmed again using BBDuk with default settings implemented in Geneious Prime [26]. The high-quality reads of *A. glabripennis* and *D. pseudonotabilis* were, respectively, mapped to the reference mitogenome of the previously sequenced *A. glabripennis* (NC_008221) [23] and amplified bilaterally by Geneious Prime [26], with the parameters set as follows: 95% minimum overlap identity, 50 bp minimum overlap, and maximum ambiguity as 4. The completeness of each circular mitogenome was confirmed when both ends of the final assembled contigs overlapped (100% coverage). The assembled mitogenomes of *A. glabripennis* and *D. pseudonotabilis* were deposited in GenBank under the accession numbers OP096420 and OP096419, respectively.

The two mitogenomes were annotated in the MITOS web server [27]. The resultant gene boundaries of the protein-coding genes (PCGs) were checked manually by the NCBI's ORF Finder (https://www.ncbi.nlm.nih.gov/orffinder/, accessed on 9 August 2022). The location and secondary structures of the transfer RNA (tRNA) and ribosomal RNA (rRNA) genes were predicted and visualized by MITOS. The mitogenome structure and GC skews were visualized by the CGView Server [28]. The nucleotide composition, skews, codon usage, and relative synonymous codon usage (RSCU) were calculated by MEGA11 [29]. The synonymous substitution rate (Ks) and nonsynonymous substitution rate (Ka) were calculated using KaKs_Calculator v2.0, with the mitogenome of *Aoria nigripes* (Baly, 1860) (Chrysomelidae) as the outgroup [30,31]. The alignment file of each PCG was uploaded to the Datamonkey web server for a more thorough exploration of selective pressure in PCGs of the two newly sequenced mitogenomes. BUSTED (Branch-Site Unrestricted Statistical Test for Episodic Diversification) was used to test whether each PCG has experienced positive selection [32]. FEL (fixed-effects likelihood) was employed to infer site-specific Ks and Ka values and detect the following four types of sites in each PCG: diversifying sites, purifying sites, neutral sites, and invariable sites [33]. Tandem repeats in the control regions were identified using the Tandem Repeats Finder web server [34]. The stem-loop structures in the control region were predicted by the Mfold web server with default settings [35].

2.3. Phylogenetic Analyses Methods

The phylogenetic relationships were reconstructed based on the nucleotide sequences of 13 PCGs derived from 186 mitogenomes of Cerambycidae *s.l.* (Table 1). Overall, 30 of the 186 mitogenomes were originally unannotated in GenBank; they were re-annotated by MITOS and manual homology alignments in this study. Other mitogenomes from GenBank that had incomplete set of 13 PCGs or incorrect PCG sequences were omitted from the dataset. The mitogenome of *A. nigripes* (Chrysomelidae) was used as the outgroup [31]. The 13 PCGs were, respectively, aligned using MUSCLE with a codon mode [36], followed by the deletion of stop codons and the concatenation of sequences by SequenceMatrix v1.7.8 [37]. The best-fit partitioning schemes and substitution models for each PCG region were determined by PartitionFinder v2.1.1 using the Bayesian information criterion (BIC) and a greedy search algorithm of all available models [38]. Phylogenies were inferred using maximum-likelihood (ML) and Bayesian inference (BI) methods. The best-fit model was GTR+I+G for two partitioned subsets: one subset included *ND1*, *ND4*, *ND4L*, and *ND5*; the other subset included the remaining 9 PCGs. IQ-Tree was used to perform the ML analysis under the edge-unlinked partition model for 5000 ultrafast bootstraps as well as the Shimodaira–Hasegawa-like approximate likelihood-ratio test [39–41]. The BI analysis was conducted by MrBayes v3.2.7 [42] with four independent Markov chains for 30 million generations and sampled every 100 generations. The first 25% of the trees were discarded as burn-in. FigTree v1.4.4 was used to edit and visualize the phylogenetic trees [43].

Table 1. Species used in this study.

Family	Subfamily	Species	Genome Size (bp)	GenBank No.
Cerambycidae *s.s.*	Cerambycinae	*Allotraeus orientalis*	15,966	NC_061181
		Anoplistes halodendri	15,697	NC_053350
		Aromia bungii	15,652	MW617355
		A. bungii	15,760	NC_053714
		A. bungii	15,759	OK393714
		Chloridolum lameeri	15,731	MN420467
		Chlorophorus annularis	15,487	NC_061058
		Chlorophorus diadema	15,398	MN473096
		Chlorophorus simillimus	13,675	KY796055
		Clytobius davidis	15,571	MN473101
		D. pseudonotabilis	15,527	OP096419
		Epipedocera atra	15,662	NC_051944
		Gnatholea eburifera	15,281	MN420473
		Jebusaea hammerschmidtii	15,619	MZ054170
		Massicus raddei	15,858	NC_023937
		Megacyllene sp. KM-2017	15,832	MG193470
		Molorchus minor	15,685	MN442323
		Nadezhdiella cantori	16,049	NC_061180
		Neoplocaederus obesus	15,683	NC_048951
		Nortia carinicollis	15,602	NC_044698
		Obrium cantharinum	15,632	MN420489
		Obrium sp. NS-2015	15,680	KT945156
		Polyzonus fasciatus	15,804	MN442321
		Purpuricenus lituratus	15,744	MN473112
		Purpuricenus temminckii	15,689	MN527358
		Pyrrhidium sanguineum	16,203	KX087339
		P. sanguineum	15,748	MN442320
		Rhytidodera bowringii	15,278	MN420472
		Semanotus bifasciatus	13,837	KY765550
		S. bifasciatus	16,051	MN095416
		Stenodryas sp. N127	15,333	MN473097
		Trichoferus campestris	13,696	KY773688
		T. campestris	15,737	MN473098
		Turanoclytus namaganensis	15,565	NC_060874
		Xoanodera maculata	15,767	NC_061182
		Xylotrechus grayii	15,540	NC_030782
		Xylotrechus magnicollis	13,692	KY773690
		Xystrocera globosa	15,707	NC_045097
		Zoodes fulguratus	15,885	MW858149
	Dorcasominae	*Apatophysis sieversi*	15,278	MN420474
		Dorcasomus pinheyi	16,040	MN447435
		Tsivoka simplicicollis	16,700	MN420488
	Lamiinae	*Acanthocinus griseus*	15,600	MN473099
		Agapanthia amurensis	15,512	MW617354
		Agapanthia daurica	14,282	KY773692
		A. daurica	17,153	MN473114
		Agelasta perplexa	15,552	NC_053905
		Anaesthetis testacea	15,169	MN420492
		Annamanum lunulatum	15,610	NC_046851
		Anoplophora chinensis	15,871	MN882586
		A. chinensis	15,805	NC_029230
		A. glabripennis	15,774	NC_008221
		Anoplophora horsfieldi	15,796	MN248534
		A. horsfieldi	15,837	NC_059864
		A. glabripennis	15,622	OP096420

Table 1. *Cont.*

Family	Subfamily	Species	Genome Size (bp)	GenBank No.
		Apomecyna saltator	14,949	NC_056277
		Apriona germarii	14,858	NC_056838
		Apriona swainsoni	15,412	NC_033872
		Aristobia reticulator	15,838	NC_042151
		Aulaconotus atronotatus	14,491	MW858150
		Batocera davidis	15,554	MN420468
		Batocera lineolata	15,420	MF521888
		B. lineolata	16,158	MW629558
		B. lineolata	15,420	MZ073344
		B. lineolata	15,418	NC_022671
		Batocera rubus	16,158	NC_062817
		Blepephaeus succinctor	15,554	NC_044697
		Cobelura sp. KM-2017	15,912	MG193463
		Epiglenea comes	15,213	MN473116
		Eutetrapha metallescens	15,072	KY796053
		Glenea cantor	15,514	NC_043883
		Glenea licenti	15,435	MN473117
		Glenea paraornata	15,510	MN420483
		Glenea relicta	15,486	MN420484
		Heteroglenea nigromaculata	15,502	MN420485
		Jamesia sp. KM-2017	17,430	MG193322
		Lamiinae sp. 1 ACP-2013	15,737	MH789723
		Lamiinae sp. 2 ACP-2013	15,440	MH789720
		Lamiinae sp. 4 ACP-2013	15,504	MH789721
		Lamiinae sp. 4 ACP-2013	15,554	MH836614
		Menesia sulphurata	15,551	MN473119
		Moechotypa diphysis	15,493	MW617356
		Monochamus alternatus	14,649	JX987292
		M. alternatus	14,189	MW858152
		M. alternatus	15,874	NC_024652
		M. alternatus	15,880	NC_050066
		Monochamus sartor urussovii	14,359	KY773691
		Monochamus sparsutus	16,029	NC_053906
		Monochamus sutor	14,350	KY773689
		Niphona lateraliplagiata	15,902	MN473100
		Oberea diversipes	15,499	NC_053945
		Oberea formosana	15,675	MN473118
		Oberea yaoshana	15,529	MK863509
		Olenecamptus bilobus	15,262	NC_051945
		Olenecamptus subobliteratus	13,854	KY796054
		Paraglenea fortunei	15,401	MN442322
		P. fortunei	15,496	NC_056837
		Parmena novaki	15,668	MN420491
		Psacothea hilaris	15,856	NC_013070
		Pseudoechthistatus chiangshunani	16,419	OP006455
		Pseudoechthistatus hei	16,103	NC_065262
		Pterolophia sp. ZJY-2019	16,063	NC_044699
		Saperda tetrastigma	15,563	MZ955033
		Serixia sedata	14,714	MN420487
		Thermistis croceocincta	15,503	NC_044700
		Thyestilla gebleri	15,503	MN420486
		T. gebleri	15,505	NC_034752
	Lepturinae	*Anastrangalia sequensi*	16,269	NC_038090
		Brachyta interrogationis	18,165	KX087246
		Cortodera humeralis	15,928	KX087264

Table 1. *Cont.*

Family	Subfamily	Species	Genome Size (bp)	GenBank No.
		Gaurotes virginea	15,775	MN473081
		Grammoptera ruficornis	16,458	MN473080
		Leptura aethiops	15,690	MN420475
		Leptura annularis	16,530	MN420469
		Leptura arcuata	14,382	KY796051
		Oxymirus cursor	15,797	MN473085
		Pachyta bicuneata	13,894	KY765551
		Peithona prionoides	13,636	MN473095
		Pidonia lurida	15,668	MN473083
		Rhagium fortecostatum	16,274	MN473103
		Rhamnusium bicolor	15,527	MN473084
		Rutpela maculata	17,437	OW386295
		Sachalinobia koltzei	15,809	MN473113
		Stenurella nigra	16,504	KX087348
		Stictoleptura succedanea	14,381	KY796052
		Teledapalpus zolotichini	16,651	MN473111
		Stenocorus meridianus	16,227	MN473082
		Xylosteus spinolae	15,708	MN473086
	Necydalinae	*Necydalis major*	15,598	MN473087
		Ulochaetes vacca	15,593	MN473110
	Parandrinae	*Papuandra araucariae*	15,475	MN420477
	Prioninae	*Aegolipton marginale*	16,759	MN420471
		Aegosoma pallidum	15,668	MN473115
		Aegosoma sinicum	15,658	KY773686
		A. sinicum	15,658	NC_038089
		Aesa media	15,714	MK614538
		Agrianome spinicollis	15,633	MK614550
		Analophus parallelus	15,722	MK614551
		Archetypus frenchi	16,156	MK614554
		Bifidoprionus rufus	15,590	MK614537
		Brephilydia jejuna	15,659	MK614541
		Cacodacnus planicollis	15,671	MK614543
		Callipogon relictus	15,742	NC_037698
		Cnemoplites australis	15,675	MK614536
		Cnemoplites edulis	13,161	MK614556
		Dorysthenes buquetii	15,778	MN420481
		Dorysthenes granulosus	15,858	MN829437
		Dorysthenes paradoxus	15,922	NC_037927
		Eboraphyllus middletoni	15,776	MK614546
		Enneaphyllus aeneipennis	16,505	MK614545
		Eurynassa australis	15,612	MK614547
		Geoffmonteithia queenslanda	15,628	MK614544
		Hermerius prionoides	13,696	MK614542
		Howea angulata	15,626	MK614532
		Megopis sinica	15,689	NC_045407
		Nepiodes costipennis multicarinatus	15,935	MN420482
		Olethrius laevipennis	15,690	MK614533
		Papunya picta	15,737	MK614539
		Paulhutchinsonia pilosicollis	15,846	NC_048496
		Phaolus metallicus	15,997	MK614535
		Phlyctenosis sp. N135	15,000	MN473102
		Priotyrannus closteroides	15,854	NC_062855
		Pseudoplites inexpectatus	15,651	MK614549
		Rhipidocerus australasiae	15,721	MK614540
		Sarmydus sp. N117	15,720	MN473091

Table 1. *Cont.*

Family	Subfamily	Species	Genome Size (bp)	GenBank No.
		Sceleocantha sp. 4 MJ-2019	15,804	MK614555
		Teispes insularis	15,632	MK614553
		Toxeutes arcuatus	15,859	MK614548
		Toxeutes macleayi	13,579	MK614559
		Tragosoma depsarium	15,712	MN473090
		Utra nitida	14,976	MK614534
		Xixuthrus sp. ANIC_25-067096	15,523	MK614552
	Spondylidinae	*Arhopalus rusticus*	15,860	MN473105
		Arhopalus unicolor	15,760	NC_053904
		Cephalallus oberthueri	15,763	NC_062854
		Saphanus piceus	15,832	MN473088
		Spondylis buprestoides	16,070	MN420476
		S. buprestoides	15,837	NC_052914
Disteniidae	Disteniinae	*Clytomelegena kabakovi*	15,816	MN473109
		Distenia gracilis	15,704	MN473106
		Disteniinae sp. BMNH 899837	15,598	KX035158
		Typodryas sp. N143	15,647	MN473107
Oxypeltidae	Oxypeltinae	*Oxypeltus quadrispinosus*	16,140	MN420465
		O. quadrispinosus	17,001	MN420466
Vesperidae	Anoplodermatinae	*Migdolus* sp. N51	14,931	MN420478
	Vesperinae	*Vesperus sanzi*	16,125	MN473093
Chrysomelidae		*A. nigripes*	17,306	ON553912

3. Results and Discussion

3.1. Genome Structure and Composition

The assembled complete mitogenomes of *A. glabripennis* and *D. pseudonotabilis* are circular DNA molecules of 15,622 bp and 15,527 bp in length (Figure 1), respectively, which is within the range of the sequenced mitogenomes of Cerambycidae in GenBank (Table 1). Due to the presence of a shorter *COX1* gene, the newly obtained *A. glabripennis* mitogenome is slightly shorter than the previously sequenced mitogenome (15,774 bp) based on samples from Hebei Province [31]. Both newly sequenced mitogenomes contain the standard set of 37 mitochondrial genes (13 PCGs, 22 tRNA genes, and 2 rRNA genes) as all other longicorn beetles. The gene order is identical to all other species of Cerambycidae as well as the ancestral mitogenome type of *Drosophila yakuba* Burla, 1954 [14,44,45]. Among the 37 genes, 23 (9 PCGs and 14 tRNAs) genes are on the majority strand (J-strand), while the remaining 4 PCGs, 8 tRNAs, and 2 rRNA genes are on the minority strand (N-strand).

A total of nine gene overlapping regions were found in the *A. glabripennis* mitogenome with a total of 29 bp in length, and the longest overlapping sequence (8 bp) was located between *trnCys* and *trnTyr*. In the *D. pseudonotabilis* mitogenome, there are 12 overlapping regions with a total of 21 bp in length, and the longest overlapping sequences were only 4 bp in length. The universally found 7 bp overlapping regions between *ATP8* and *ATP6*, as well as *NAD4* and *NAD4L* in Cerambycidae and many other insects [14,15], are restricted to the overlapping between *NAD4* and *NAD4L* in the *A. glabripennis* mitogenome, which might be resulted from the different annotation methods. In addition to the overlapping regions, multiple intergenic spacers are scattered throughout both mitogenomes (Tables 2 and 3). The base composition is 38.8% A, 14.2% C, 9.2% G, and 37.8% T for the *A. glabripennis* mitogenome and 39.7% A, 14.5% C, 10.5% G, and 35.3% T for *D. pseudonotabilis*. The two mitogenomes are highly skewed towards A and T nucleotides, with an A + T content of 76.6% in *A. glabripennis* and 75.0% in *D. pseudonotabilis* (Table 1).
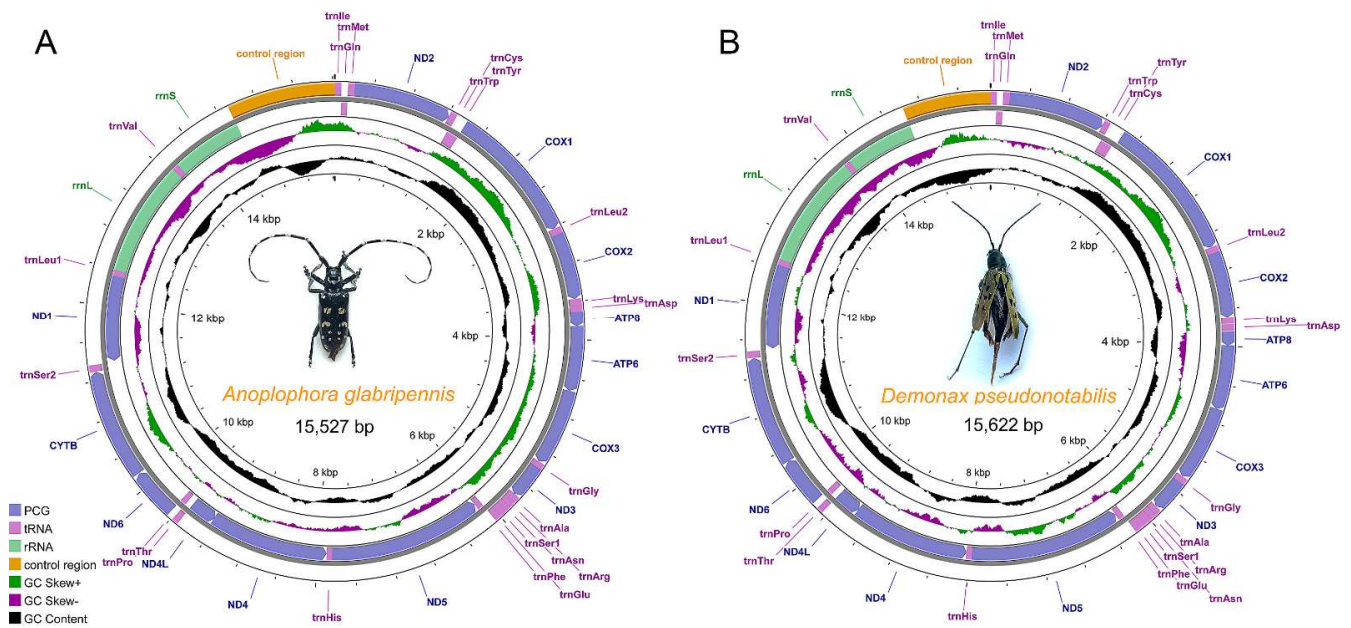
Figure 1. Mitochondrial genome maps of *A. glabripennis* (**A**) and *D. pseudonotabilis* (**B**). Genes outside the map are transcribed clockwise, whereas those inside the map are transcribed counterclockwise. The inside circles show the GC content and the GC skew. GC content and GC skew are plotted as the deviation from the average value of the entire sequence.

Table 2. Mitochondrial genome organization of *A. glabripennis*.

Gene	Position (bp)	Size (bp)	Direction	Intergenic Nucleotides	Anti− or Start/Stop Codons	A + T%
trnIle (I)	1–67	67	Forward	0	GAT	61.2
trnGln (Q)	69–137	69	Reverse	1	TTG	78.3
trnMet (M)	137–205	69	Forward	−1	CAT	72.5
ND2	206–1216	1011	Forward	0	ATT/TAA	77.6
trnTrp (W)	1215–1282	68	Forward	−2	TCA	76.5
trnCys (C)	1275–1336	62	Reverse	−8	GCA	74.2
trnTyr (Y)	1338–1402	65	Reverse	1	GTA	69.2
COX1	1403–2819	1417	Forward	0	ATC/T	68.1
trnLeu2 (L2)	2820–2884	65	Forward	0	TAA	73.8
COX2	2885–3572	688	Forward	0	ATC/T	72.1
trnLys (K)	3573–3641	69	Forward	0	CTT	68.1
trnAsp (D)	3642–3707	66	Forward	0	GTC	86.4
ATP8	3708–3863	156	Forward	0	ATT/TAG	86.5
ATP6	3860–4531	672	Forward	−4	ATA/TAA	75.1
COX3	4531–5319	789	Forward	−1	ATG/TAA	70.6
trnGly (G)	5322–5385	64	Forward	2	TCC	85.9
ND3	5383–5739	357	Forward	−3	ATA/TAG	79.0
trnAla (A)	5738–5802	65	Forward	−2	TGC	81.5
trnArg (R)	5803–5864	62	Forward	0	TCG	74.2
trnAsn (N)	5864–5927	64	Forward	−1	GTT	75.0
trnSer1 (S1)	5928–5994	67	Forward	0	GCT	76.1
trnGlu (E)	5995–6057	63	Forward	0	TTC	87.3
trnPhe (F)	6060–6123	64	Reverse	2	GAA	82.8
ND5	6124–7840	1717	Reverse	0	ATT/T	78.3
trnHis (H)	7841–7903	63	Reverse	0	GTG	84.1
ND4	7904–9236	1333	Reverse	0	ATG/T	79.3
ND4L	9230–9517	288	Reverse	−7	ATG/TAA	83.0
trnThr (T)	9520–9583	64	Forward	2	TGT	82.8

Table 2. *Cont.*

Gene	Position (bp)	Size (bp)	Direction	Intergenic Nucleotides	Anti− or Start/Stop Codons	A + T%
trnPro (P)	9584–9647	64	Reverse	0	TGG	78.1
ND6	9650–10,153	504	Forward	2	ATT/TAA	85.1
CYTB	10,159–11,292	1134	Forward	5	ATA/TAA	72.2
trnSer2 (S2)	11,296–11,364	69	Forward	3	TGA	81.2
ND1	11,382–12,332	951	Reverse	17	TTG/TAG	76.3
trnLeu1 (L1)	12,334–12,398	65	Reverse	1	TAG	78.5
rrnL	12,399–13,670	1272	Reverse	0		80.1
trnVal (V)	13,671–13,739	69	Reverse	0	TAC	75.4
rrnS	13,740–14,518	779	Reverse	0		78.6
Control Region	14,519–15,622	1104	Forward	0		79.3

Table 3. Mitochondrial genome organization of *D. pseudonotabilis*.

Gene	Position (bp)	Size (bp)	Direction	Intergenic Nucleotides	Anti− or Start/Stop Codons	A + T%
trnIle (I)	1–66	66	Forward	0	GAT	72.7
trnGln (Q)	64–132	69	Reverse	−3	TTG	81.2
trnMet (M)	132–200	69	Forward	−1	CAT	65.2
ND2	201–1211	1011	Forward	0	ATA/TAA	76.2
trnTrp (W)	1210–1274	65	Forward	−2	TCA	73.8
trnCys (C)	1274–1339	66	Reverse	−1	GCA	72.7
trnTyr (Y)	1341–1405	65	Reverse	1	GTA	66.2
COX1	1440–2940	1501	Forward	34	ATT/T	67.0
trnLeu2 (L2)	2941–3005	65	Forward	0	TAA	72.3
COX2	3006–3692	687	Forward	0	ATA/TAT	70.7
trnLys (K)	3694–3764	71	Forward	1	CTT	70.4
trnAsp (D)	3768–3837	70	Forward	3	GTC	82.9
ATP8	3847–3993	147	Forward	9	ATA/TAG	85.0
ATP6	3990–4661	672	Forward	−4	ATA/TAA	74.3
COX3	4661–5447	787	Forward	−1	ATG/T	69.5
trnGly (G)	5448–5510	63	Forward	0	TCC	84.1
ND3	5511–5862	352	Forward	0	ATT/T	76.1
trnAla (A)	5863–5925	63	Forward	0	TGC	77.8
trnArg (R)	5925–5989	65	Forward	−1	TCG	73.8
trnAsn (N)	5989–6053	65	Forward	−1	GTT	73.8
trnSer1 (S1)	6054–6120	67	Forward	0	GCT	74.6
trnGlu (E)	6121–6186	66	Forward	0	TTC	86.4
trnPhe (F)	6190–6256	67	Reverse	3	GAA	79.1
ND5	6257–7973	1717	Reverse	0	ATT/T	77.4
trnHis (H)	7974–8037	64	Reverse	0	GTG	84.4
ND4	8037–9368	1332	Reverse	−1	ATA/TAA	76.4
ND4L	9365–9643	279	Reverse	−4	ATG/TAA	79.9
trnThr (T)	9646–9709	64	Forward	2	TGT	84.4
trnPro (P)	9709–9774	66	Reverse	−1	TGG	75.8
ND6	9776–10,273	498	Forward	1	ATA/TAA	81.7
CYTB	10,273–11,409	1137	Forward	−1	ATG/TAA	68.1
trnSer2 (S2)	11,411–11,479	69	Forward	1	TGA	78.3
ND1	11,497–12,447	951	Reverse	17	TTG/TAG	75.8
trnLeu1 (L1)	12,449–12,512	64	Reverse	1	TAG	75.0
rrnL	12,513–13,778	1266	Reverse	0		78.8
trnVal (V)	13,779–13,846	68	Reverse	0	TAC	77.9
rrnS	13,847–14,620	774	Reverse	0		76.5
Control Region	14,621–15,527	907	Forward	0		82.1

3.2. Protein-Coding Genes

The PCGs have identical arrangement and similar size between the two mitogenomes and also other cerambycids. Most PCGs of the two species start with the standard ATN start codons (ATA, ATC, ATG, and ATT), whereas *ND1* of both mitogenomes begins with the special codon TTG (Tables 2 and 3), which was similar to all other published Cerambycidae mitogenomes [14,15]. Most PCGs of each mitogenome have the complete termination codon TAN (TAA, TAT, or TAG), whereas four PCGs (*COX1*, *COX2*, *ND4*, and *ND5*) of *A. glabripennis* and four PCGs (*COX1*, *COX3*, *ND3*, and *ND5*) of *D. pseudonotabilis* end with an incomplete stop codon T. These incomplete stop codons are considered to be caused by the post-transcriptional polyadenylation [46] and can be completed by the addition of 3′ nucleotide residues to the neighboring mitochondrial genes.

The relative synonymous codon usage (RSCU) values indicate the most frequently used codon is TTA (Leu) for both mitogenomes (Figure 2), which appears to be a common feature of other sequenced longicorn beetles [14]. *ATP8* of both mitogenomes has the highest A + T content among the 13 PCGs (Tables 2 and 3). The Ka/Ks ratios for each PCG of each mitogenome are calculated to assess the selective pressure of the two cerambycid species (Figure 3A). The evolutionary rate of *ND6* was the highest among the 13 PCGs. The Ka/Ks ratios of all the 13 PCGs calculated by KaKs_Calculator v2.0 were below 1, which suggests the existence of purifying selection in the two species (Figure 3A). The results of Ka/Ks calculation were similar to a recent mitogenomic work [47], which used DnaSP for the calculation. The gene-wide BUSTED analysis based on the likelihood-ratio test found no evidence of episodic diversifying selection in the PCGs. The site-specific FEL analysis detected *ND4* and *ND4L* each had one codon site under diversifying positive selection at $p \leq 0.1$ (Figure 3B). Nearly one-third of each PCG's codon sites were under purifying selection at $p \leq 0.1$. The calculation of KaKs_Calculator v2.0 was consistent with the results of FEL analysis that the PCGs with lower Ka/Ks ratios tended to have more purifying codon sites (Figure 3).

3.3. Transfer RNAs, Ribosomal RNAs, and Control Region

The two mitogenomes both contain the complete set of 22 tRNA genes typical of metazoan mitogenomes. These tRNAs range in size from 62 to 69 bp, which was consistent with previously sequenced mitogenomes of Cerambycidae [15]. The highest A + T content is found in *trnGlu* of both mitogenomes (Tables 2 and 3). Most of the tRNAs have typical cloverleaf secondary structures, whereas the dihydrouridine (DHU) arm of *trnSer1* is shortened in both mitogenomes (Figure 4), which is a common phenomenon in hexapods and metazoan mitogenomes [48]. Numerous mismatched base pairs are found in the secondary structures of tRNA genes, and all of them are G–U pairs.

The large ribosomal RNA (*rrnL*) gene and small ribosomal RNA (*rrnS*) gene are found in the conserved location between *trnLeu1* and the control region (Tables 2 and 3). The *rrnL* gene is 1272 bp long in *A. glabripennis* and 1266 bp long in *D. pseudonotabilis*, with an A + T content of 80.1% and 78.8%, respectively. The *rrnS* gene is 779 bp long in *A. glabripennis* and 774 bp long in *D. pseudonotabilis*, with an A + T content of 78.6% and 76.5%, respectively.

The control region (CR) is the longest non-coding area in the two mitogenomes (Figure 1) and is functional in the regulation, transcription, and replication processes of the mitogenomes [49]. The CR of *A. glabripennis* is 1104 bp long and has an A + T content of 79.3%; the CR of *D. pseudonotabilis* is 907 bp long and has an A + T content of 82.1% (Tables 2 and 3). In the CR of *A. glabripennis*, 5.2 copies of 57 bp long tandem repeat "AAAATTTCATCAGCTAGCTCCGCTATATAAAATCGCCTACCTTTCAAATTTCC-CCTA" are detected near the 5′ end of this region. A total of 22 standard (single stem with single loop) and another 7 more complicated stem-loop structures are predicted in the CR of *A. glabripennis* (Figure S1). There are 17 standard and 4 complicated stem-loop structures in the CR of *D. pseudonotabilis* (Figure S2). However, no tandem repeats are found in the CR of *D. pseudonotabilis*. Functions of these secondary structures are unclear.
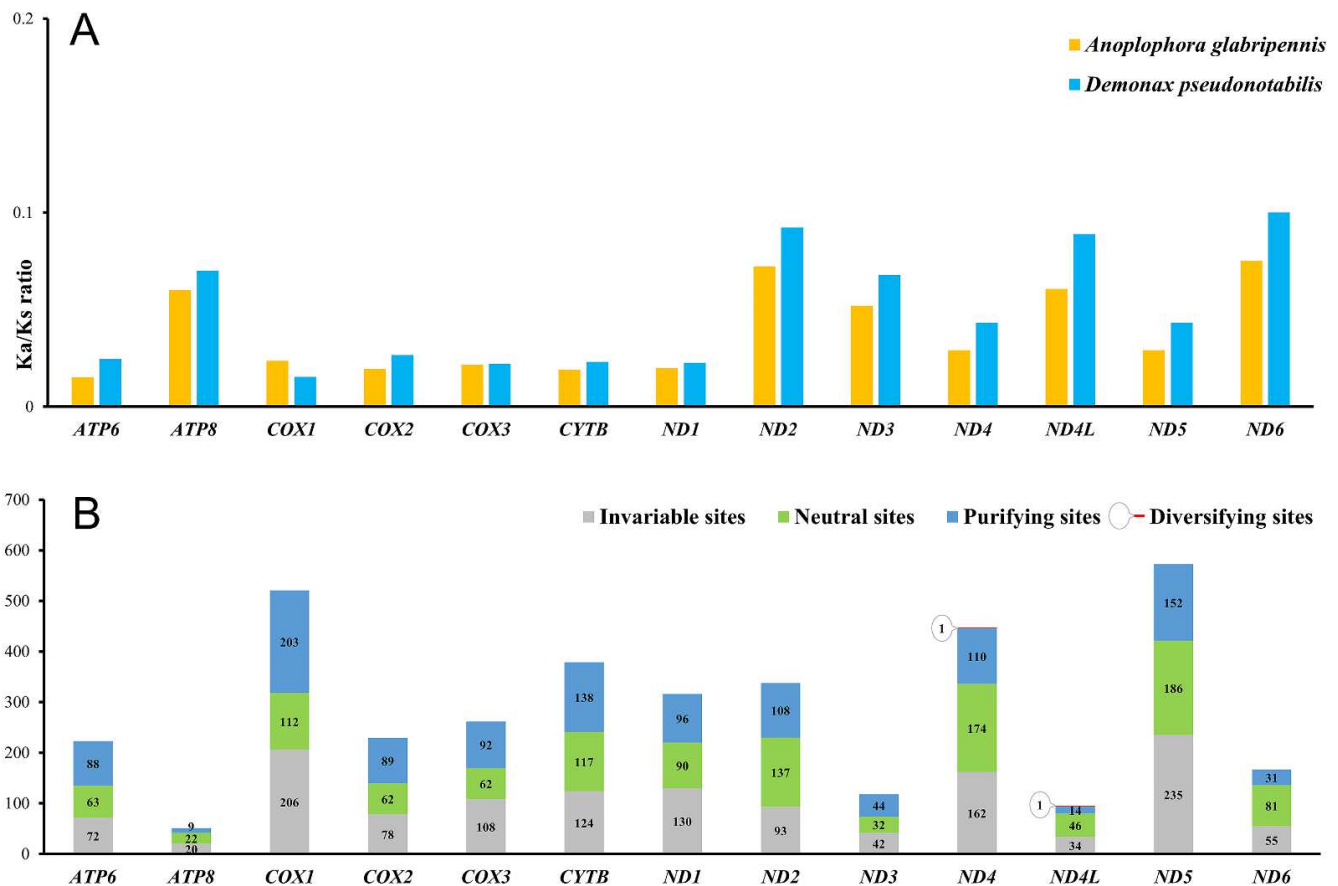
Figure 2. Relative synonymous codon usage (RSCU) of PCGs in *A. glabripennis* (**A**) and *D. pseudonotabilis* (**B**).

Figure 3. Nonsynonymous/synonymous substitution ratios (**A**) and codon sites diversity (**B**) of mitochondrial PCGs of *A. glabripennis* and *D. pseudonotabilis*.

3.4. Phylogenetic Analyses

The phylogenetic positions of *A. glabripennis* and *D. pseudonotabilis* are reconstructed based on the combined mitochondrial gene set of 13 PCGs. The ML and BI analyses generated similar tree topology (Figures 5 and S3). The phylogenetic results are largely congruent with the recent comprehensive mitogenomic phylogenetic study of Nie et al. (2020) [15]. The monophyly of Cerambycidae *s.s.* is not well-supported in both ML and BI trees due to the inclusion of other families of Chrysomeloidea (Figure 5), which is similar to the results of Haddad et al. (2018) [5] and Nie et al. (2020) [15]. The positions of Disteniidae and Oxypeltidae are variable, and Oxypeltidae is recovered as the sister group to all other taxa in the BI tree (Figure S3). The phylogenetic position of Disteniidae remains uncertain, and this family has been recovered as the sister group to various other members of Cerambycidae *s.l.* based on either molecular or morphological datasets [5,9,15,50–57]. The monophyly of Cerambycidae *s.s.* is still one of the most debatable subjects in the phylogeny and evolution of Chrysomeloidea [5].

The monophyly of Cerambycinae, Dorcasominae, Lamiinae, and Necydalinae is well-supported in both ML and BI analyses (Figures 5 and S3). The subfamily Parandrinae is placed within Prioninae and should be treated as a tribe of Prioninae, as suggested in previous studies [15,58]. Similarly, Necydalinae is nested in Lepturinae and should be regarded as a tribe of Lepturinae [15,50]. Spondylidinae is rendered paraphyletic by the species of Vesperidae, which differs from the monophyletic condition in Haddad et al. (2018) [5] and Nie et al. (2020) [15]. The non-monophyletic condition of Vesperidae has also been recovered based on morphological and molecular characters [54,55,59–61]. The two species sequenced in this study are, respectively, grouped with their relatives from the same subfamily.

Although numerous contributions have been made to explore the higher-level phylogeny of longhorn beetles, there are still some debatable points to be solved: the monophyly of Cerambycidae *s.l.* and *s.s.*; the relative relationship between Cerambycidae *s.s.*, Disteniidae, Oxypeltidae, and Vesperidae; and the monophyly and relationship of subfamilies in Cerambycidae *s.l.*, especially within Cerambycidae *s.s.* The incongruence between different molecular phylogenetic studies could be attributed to the usage of different molecular types, sample sizes, and analytical methods. The taxonomic misidentification of sequenced samples in online databases such as GenBank could also lead to bizarre tree topology, especially for those clades with few taxa. Most main clades of Cerambycidae *s.l.* still lack sufficient molecular data to clarify their phylogenetic positions. The sequencing of more mitogenomes, optimization of datasets and substitution models, and the supplement of nuclear genes are expected to improve the resolution of mitochondrial phylogenetic reconstruction of Cerambycidae *s.l.* in future works.
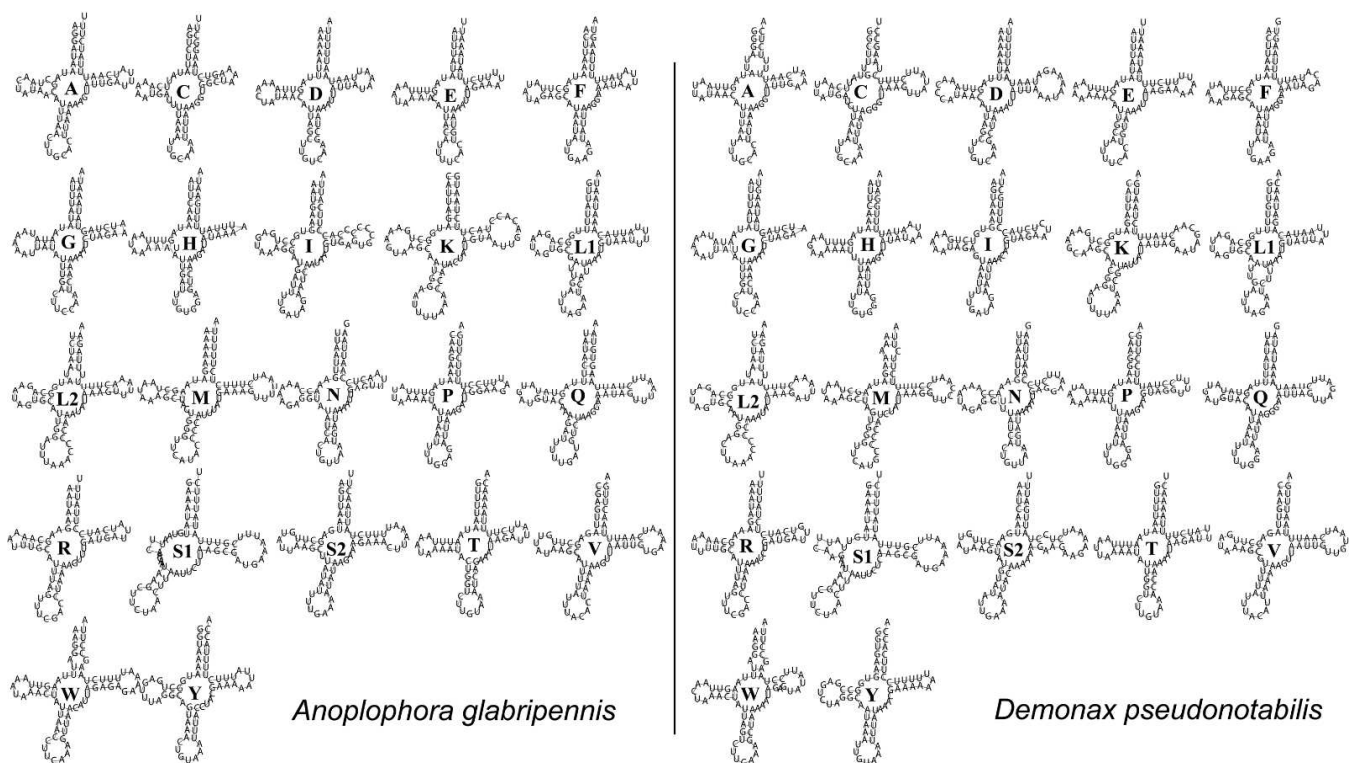

Figure 4. Secondary structures of tRNA genes in the mitogenomes of *A. glabripennis* and *D. pseudonotabilis*. The identity of each tRNA gene is represented by the abbreviation of the related amino acid.

Figure 5. Maximum-likelihood phylogeny of Cerambycidae *s.l.* inferred from mitogenomic data. Numbers at the nodes are bootstrap values.

4. Conclusions

In this study, we sequenced and analyzed the mitogenomes of two longicorn beetles, which are important pests of cultivated ecosystems in China. The structure and content of the two mitogenomes are conserved in comparison to other sequenced mitogenomes of

Cerambycidae, but the intraspecific mitogenomic variation is also detected. The monophyly of four subfamilies was supported by the phylogenetic analysis based on the nucleotide sequence of PCGs. The results provided basic genetic information for understanding the phylogeny and evolution of longicorn beetles.

Supplementary Materials: The following supporting information can be downloaded at: https://www.mdpi.com/article/10.3390/genes13101881/s1, Figure S1: Predicted stem-loop structures in the control region of *A. glabripennis*; Figure S2: Predicted stem-loop structures in the control region of *D. pseudonotabilis*; Figure S3: Bayesian inference phylogeny of Cerambycidae *s.l.* inferred from mitogenomic data. Numbers at the nodes are posterior probabilities.

Author Contributions: Conceptualization and original draft, D.-Q.P.; data curation and methodology, H.-L.L. and X.-L.W.; writing—review and editing, Z.-T.C. All authors have read and agreed to the published version of the manuscript.

Institutional Review Board Statement: No special permits were required to retrieve and process the samples because the study did not involve any live vertebrates or regulated invertebrates.

Informed Consent Statement: Not applicable.

Data Availability Statement: The data presented in this study are available in NCBI GenBank (Accession numbers: OP096420 and OP096419).

Conflicts of Interest: The authors declare no conflict of interest.

References

1. Svacha, P.; Wang, J.J.; Chen, S.C. Larval morphology and biology of *Philus antennatus* and *Heterophilus punctulatus*, and systematic position of the Philinae (*Coleoptera*: *Cerambycidae* and *Vesperidae*). *Ann. Soc. Entomol. Fr.* **1997**, *33*, 323–369.
2. Sama, G.; Buse, J.; Orbach, E.; Friedman, A.; Rittner, O.; Chikatunov, V. A new catalogue of the *Cerambycidae* (*Coleoptera*) of Israel with notes on their distribution and host plants. *Munis Entomol. Zool.* **2010**, *5*, 1–55. [CrossRef]
3. Tavakilian, G.L.; Chevillotte, H. Titan: Base de Données Internationales sur les *Cerambycidae* ou *Longicornes*. Version 4.0. Available online: http://titan.gbif.fr (accessed on 1 August 2022).
4. Svacha, P.; Lawrence, J.F. 2.1. Vesperidae Mulsant, 1839; 2.2 Oxypeltidae Lacordaire, 1868; 2.3 Disteniidae J. Thomson, 1861; 2.4 Cerambycidae Latreille, 1802. Handbook of Zoology, Band 4: Arthropoda: Insecta, Teilband/part 40 Coleoptera, Beetles. In *Vol. 3: Morphology and Systematics (Phytophaga)*; Leschen, R.A.B., Beutel, R.G., Eds.; Walter de Gruyter: Berlin, Germany, 2014; pp. 16–177.
5. Haddad, S.; Shin, S.; Lemmon, A.R.; Lemmon, E.M.; Svacha, P.; Farrell, B.; Ślipiński, A.; Windsor, D.; McKenna, D.D. Anchored hybrid enrichment provides new insights into the phylogeny and evolution of longhorned beetles (*Cerambycidae*). *Syst. Entomol.* **2018**, *43*, 68–89. [CrossRef]
6. Monné, M.L.; Monné, M.A.; Mermudes, J.R.M. Inventário das espécies de Cerambycinae (*Insecta*, *Coleoptera*, *Cerambycidae*) do Parque Nacional do Itatiaia, RJ, Brasil. *Biota Neotrop.* **2009**, *9*, 283–312. [CrossRef]
7. Cherepanov, A.I. *Cerambycidae of Northern Asia (Prioninae, Disteniinae, Lepturinae, Aseminae)*; Nauka: Novosibirsk, Russia, 1979.
8. Švácha, P.; Danilevsky, M.L. Cerambycoid larvae of Europe and Soviet Union (*Coleoptera*, *Cerambycidae*). Part I. *Acta Univ. Carol. Biol.* **1986**, *30*, 1–176.
9. Švácha, P.; Danilevsky, M.L. Cerambycoid larvae of Europe and Soviet Union (*Coleoptera*, *Cerambycidae*). Part II. *Acta Univ. Carol. Biol.* **1987**, *31*, 121–284.
10. Švácha, P.; Danilevsky, M.L. Cerambycoid larvae of Europe and Soviet Union (*Coleoptera*, *Cerambycidae*). Part III. *Acta Univ. Carol. Biol.* **1988**, *32*, 1–205.
11. Linsley, E.G. Ecology of Cerambycidae. *Annu. Rev. Entomol.* **1959**, *4*, 99–138. [CrossRef]
12. Nowak, D.J.; Pasek, J.E.; Sequeira, R.A.; Crane, D.E.; Mastro, V.C. Potential effect of *Anoplophora glabripennis* (*Coleoptera*: *Cerambycidae*) on urban trees in the United States. *J. Econ. Entomol.* **2001**, *94*, 116–122. [CrossRef]
13. Haddad, S.; Mckenna, D.D. Phylogeny and evolution of the superfamily *Chrysomeloidea* (*Coleoptera*: *Cucujiformia*). *Syst. Entomol.* **2016**, *41*, 697–716. [CrossRef]
14. Wang, J.; Dai, X.Y.; Xu, X.D.; Zhang, Z.Y.; Yu, D.N.; Storey, K.B.; Zhang, J.Y. The complete mitochondrial genomes of five longicorn beetles (*Coleoptera*: *Cerambycidae*) and phylogenetic relationships within *Cerambycidae*. *PeerJ* **2019**, *7*, e7633. [CrossRef] [PubMed]

15. Nie, R.; Vogler, A.P.; Yang, X.K.; Lin, M. Higher-level phylogeny of longhorn beetles (*Coleoptera*: *Chrysomeloidea*) inferred from mitochondrial genomes. *Syst. Entomol.* **2021**, *46*, 56–70. [CrossRef]

16. Cameron, S.L. Insect mitochondrial genomics: Implications for evolution and phylogeny. *Annu. Rev. Entomol.* **2014**, *59*, 95–117. [CrossRef]

17. Timmermans, M.J.; Barton, C.; Haran, J.; Ahrens, D.; Culverwell, C.L.; Ollikainen, A.; Dodsworth, S.; Foster, P.G.; Bocak, L.; Vogler, A.P. Family-level sampling of mitochondrial genomes in Coleoptera: Compositional heterogeneity and phylogenetics. *Genome Biol. Evol.* **2016**, *8*, 161–175. [CrossRef] [PubMed]

18. Linard, B.; Crampton-Platt, A.; Moriniere, J.; Timmermans, M.J.; Andújar, C.; Arribas, P.; Miller, K.E.; Lipecki, J.; Favreau, E.; Hunter, A.; et al. The contribution of mitochondrial metagenomics to large-scale data mining and phylogenetic analysis of Coleoptera. *Mol. Phylogenet. Evol.* **2018**, *128*, 1–11. [CrossRef]

19. Timmermans, M.J.; Lees, D.C.; Simonsen, T.J. Towards a mitogenomic phylogeny of Lepidoptera. *Mol. Phylogenet. Evol.* **2014**, *79*, 169–178. [CrossRef]

20. Li, H.; Leavengood, J.M., Jr.; Chapman, E.G.; Burkhardt, D.; Song, F.; Jiang, P.; Liu, J.; Zhou, X.; Cai, W. Mitochondrial phylogenomics of Hemiptera reveals adaptive innovations driving the diversification of true bugs. *Proc. Biol. Sci.* **2017**, *284*, 20171223. [CrossRef]

21. Motschulsky, V. Diagnoses de Coléoptères nouveaux, trouvés par M. M. Tatarinoff et Gaschkéwitsh aux environs de Pékin. *Etud. Ent.* **1854**, *2*, 44–51.

22. Gressitt, J.L.; Rondon, J.A.; von Breuning, S. *Cerambycid-Beetles of Laos. Pacific Insects Monograph 24*; Bishop Museum: Honolulu, HI, USA, 1970.

23. Fang, J.; Qian, L.; Xu, M.; Yang, X.; Wang, B.; An, Y. The complete nucleotide sequence of the mitochondrial genome of the Asian longhorn beetle, *Anoplophora glabripennis* (*Coleoptera*: *Cerambycidae*). *Mitochondrial DNA Part A* **2016**, *27*, 3299–3300. [CrossRef]

24. Liu, H.L.; Chen, S.; Chen, Q.D.; Pu, D.Q.; Chen, Z.T.; Liu, Y.Y.; Liu, X. The first mitochondrial genomes of the family *Haplodiplatyidae* (*Insecta*: *Dermaptera*) reveal intraspecific variation and extensive gene rearrangement. *Biology* **2022**, *11*, 807. [CrossRef]

25. Chen, S.; Zhou, Y.; Chen, Y.; Gu, J. Fastp: An ultra-fast all-in-one FASTQ preprocessor. *Bioinformatics* **2018**, *34*, 884–890. [CrossRef] [PubMed]

26. Kearse, M.; Moir, R.; Wilson, A.; Stones-Havas, S.; Cheung, M.; Sturrock, S.; Buxton, S.; Cooper, A.; Markowitz, S.; Duran, C.; et al. Geneious Basic: An integrated and extendable desktop software platform for the organization and analysis of sequence data. *Bioinformatics* **2012**, *28*, 1647–1649. [CrossRef]

27. Bernt, M.; Donath, A.; Jühling, F.; Externbrink, F.; Florentz, C.; Fritzsch, G.; Pütz, J.; Middendorf, M.; Stadler, P.F. MITOS: Improved de novo metazoan mitochondrial genome annotation. *Mol. Phylogenet. Evol.* **2013**, *69*, 313–319. [CrossRef] [PubMed]

28. Grant, J.R.; Stothard, P. The CGView server: A comparative genomics tool for circular genomes. *Nucleic Acids Res.* **2008**, *36*, 181–184. [CrossRef] [PubMed]

29. Tamura, K.; Stecher, G.; Kumar, S. MEGA11: Molecular evolutionary genetics analysis version 11. *Mol. Biol. Evol.* **2021**, *38*, 3022–3027. [CrossRef]

30. Wang, D.; Zhang, Y.; Zhang, Z.; Zhu, J.; Yu, J. KaKs_Calculator 2.0: A toolkit incorporating γ-series methods and sliding window strategies. *Genom. Broteom. Bioinform.* **2010**, *8*, 77–80. [CrossRef]

31. Baly, J.S. Descriptions of new genera and species of *Eumolpidae*. *J. Entomol.* **1860**, *1*, 23–36. [CrossRef]

32. Murrell, B.; Weaver, S.; Smith, M.D.; Wertheim, J.O.; Murrell, S.; Aylward, A.; Eren, K.; Pollner, T.; Martin, D.P.; Smith, D.M.; et al. Gene-wide identification of episodic selection. *Mol. Biol. Evol.* **2015**, *32*, 1365–1371. [CrossRef]

33. Murrell, B.; Wertheim, J.O.; Moola, S.; Weighill, T.; Scheffler, K.; Kosakovsky Pond, S.L. Detecting individual sites subject to episodic diversifying selection. *PLoS Genet.* **2012**, *8*, e1002764. [CrossRef]

34. Benson, G. Tandem repeats finder: A program to analyze DNA sequences. *Nucleic Acids Res.* **1999**, *27*, 573–580. [CrossRef]

35. Zuker, M. Mfold web server for nucleic acid folding and hybridization prediction. *Nucleic Acids Res.* **2003**, *31*, 3406–3415. [CrossRef] [PubMed]

36. Edgar, R.C. MUSCLE: Multiple sequence alignment with high accuracy and high throughput. *Nucleic Acids Res.* **2004**, *32*, 1792–1797. [CrossRef] [PubMed]

37. Vaidya, G.; Lohman, D.J.; Meier, R. SequenceMatrix: Concatenation software for the fast assembly of multi-gene datasets with character set and codon information. *Cladistics* **2011**, *27*, 171–180. [CrossRef]

38. Lanfear, R.; Frandsen, P.B.; Wright, A.M.; Senfeld., T.; Calcott., B. PartitionFinder 2: New methods for selecting partitioned models of evolution for molecular and phylogenetic analyses. *Mol. Biol. Evol.* **2016**, *34*, 772–773. [CrossRef] [PubMed]

39. Minh, B.Q.; Schmidt, H.A.; Chernomor, O.; Schrempf, D.; Woodhams, M.D.; Von Haeseler, A.; Lanfear, R. IQ-TREE 2: New models and efficient methods for phylogenetic inference in the genomic era. *Mol. Biol. Evol.* **2020**, *37*, 1530–1534. [CrossRef]

40. Minh, B.Q.; Nguyen, M.A.; von Haeseler, A. Ultrafast approximation for phylogenetic bootstrap. *Mol. Biol. Evol.* **2013**, *30*, 1188–1195. [CrossRef]

41. Guindon, S.; Dufayard, J.F.; Lefort, V.; Anisimova, M.; Hordijk, W.; Gascuel, O. New algorithms and methods to estimate maximum-likelihood phylogenies: Assessing the performance of PhyML 3.0. *Syst. Biol.* **2010**, *59*, 307–321. [CrossRef]

42. Ronquist, F.; Huelsenbeck, J.P. MrBayes 3: Bayesian phylogenetic inference under mixed models. *Bioinformatics* **2003**, *19*, 1572–1574. [CrossRef]

43. Rambaut, A. FigTree Version 1.4.4. 2019. Available online: http://tree.bio.ed.ac.uk/software/fgtree/ (accessed on 8 August 2022).

44. Burla, H. Zur Kenntnis der Drosophiliden der Elfenbeinkuste (Franzosisch West-Afrika). *Rev. Suisse Zool.* **1954**, *61*, 1–218. [CrossRef]

45. Clary, D.O.; Wolstenholme, D.R. The ribosomal RNA genes of *Drosophila* mitochondrial DNA. *Nucleic Acids Res.* **1985**, *13*, 4029–4045. [CrossRef]

46. Ojala, D.; Montoya, J.; Attardi, G. tRNA punctuation model of RNA processing in human mitochondria. *Nature* **1981**, *290*, 470–474. [CrossRef] [PubMed]

47. Guo, Q.; Liu, L.; Huang, W.; Sang, W.; Chen, X.; Wang, X. Characterization of the complete mitogenome of *Trachylophus sinensis* (*Coleoptera*: *Cerambycidae*: *Cerambycinae*), the type species of *Trachylophus* and its phylogenetic implications. *J. Asia-Pac. Entomol.* **2022**, *25*, 101977. [CrossRef]

48. Garey, J.R.; Wolstenholme, D.R. Platyhelminth mitochondrial DNA: Evidence for early evolutionary origin of a tRNAserAGN that contains a dihydrouridine arm replacement loop, and of serine-specifying AGA and AGG codons. *J. Mol. Evol.* **1989**, *28*, 374–387. [CrossRef] [PubMed]

49. Zhang, D.X.; Hewitt, G.M. Insect mitochondrial control region: A review of its structure, evolution and usefulness in evolutionary studies. *Biochem. Syst. Ecol.* **1997**, *25*, 99–120. [CrossRef]

50. Linsley, E.G.; Chemsak, J.A. The Cerambycidae of North America, part VI, no. 1. Taxonomy and classification of the subfamily *Lepturinae*. *Univ. Calif. Publ. Entomol.* **1972**, *69*, 1–138.

51. Crowson, R.A. *The Biology of the Coleoptera*; Academic Press: London, UK, 1981.

52. Gómez-Zurita, J.; Hunt, T.; Kopliku, F.; Vogler, A.P. Recalibrated tree of leaf beetles (*Chrysomelidae*) indicates independent diversification of angiosperms and their insect herbivores. *PLoS ONE* **2007**, *2*, e360. [CrossRef]

53. Hunt, T.; Bergsten, J.; Levkanicova, Z.; Papadopoulou, A.; John, O.S.; Wild, R.; Hammond, P.M.; Ahrens, D.; Balke, M.; Caterino, M.S.; et al. A comprehensive phylogeny of beetles reveals the evolutionary origins of a superradiation. *Science* **2007**, *318*, 1913–1916. [CrossRef]

54. Lawrence, J.F.; Ślipiski, A.; Seago, A.E.; Thayer, M.K.; Newton, A.F.; Marvaldi, A.E. Phylogeny of the Coleoptera based on morphological characters of adults and larvae. *Ann. Zool.* **2011**, *61*, 1–217. [CrossRef]

55. Mckenna, D.D.; Wild, A.L.; Kanda, K.; Bellamy, C.L.; Beutel, R.G.; Caterino, M.S.; Farnum, C.W.; Hawks, D.C.; Ivie, M.A.; Jameson, M.L.; et al. The beetle tree of life reveals Coleoptera survived end Permian mass extinction to diversify during the cretaceous terrestrial revolution. *Syst. Entomol.* **2015**, *40*, 835–880. [CrossRef]

56. Wang, B.; Ma, J.Y.; McKenna, D.D.; Yan, E.V.; Zhang, H.C.; Jarzembowski, E.A. The earliest known longhorn beetle (*Cerambycidae*: *Prioninae*) and implications for the early evolution of *Chrysomeloidea*. *J. Syst. Palaeontol.* **2014**, *12*, 565–574. [CrossRef]

57. Wei, Z.H.; Yin, X.M.; An, S.H.; Su, L.J.; Li, J.; Zhang, H.F. Molecular phylogenetic study of the higher taxa of the superfamily *Cerambycoidea* (*Insecta*: *Coleoptera*) based on the combined analysis of ribosomal DNA sequences. *Acta Entomol. Sin.* **2014**, *57*, 710–720.

58. Danilevsky, M.L. *Morpho-Adaptive Ways of Evolution of the Larvae of Longhorn Beetles (Coleoptera, Cerambycidae) and Phylogenetic Relations of the Basic Groups of the Family. Insects Decomposing Wood and their Entomophages*; Nauka: Moscow, Russia, 1979.

59. Napp, D.S. Phylogenetic relationships among the subfamilies of *Cerambycidae* (*Coleoptera*, *Chrysomeloidea*). *Rev. Bras. Entomol.* **1994**, *28*, 265–419.

60. Reid, C.A.M. A cladistic analysis of subfamilial relationships in the *Chrysomelidae* sensu lato (*Chrysomeloidea*). In *Biology, Phylogeny and Classification of Coleoptera: Papers Celebrating the 80th Birthday of Roy A. Crowson*; Pakaluk, J., Slipinski, S.A., Eds.; Muzeum i Instytut Zoologii Polska Akademia Nauk: Warsaw, Poland, 1995; pp. 559–632.

61. Bocak, L.; Barton, C.; Crampton-Platt, A.; Chesters, D.; Ahrens, D.; Vogler, A.P. Building the Coleoptera tree-of-life for >8000 species: Composition of public DNA data and fit with Linnaean classification. *Syst. Entomol.* **2014**, *39*, 97–110. [CrossRef]